

Multistage Stochastic Investment Planning with Multiscale Representation of Uncertainties and Decisions

Yixian Liu, Ramteen Sioshansi, *Senior Member, IEEE*, and Antonio J. Conejo, *Fellow, IEEE*

Abstract—We propose a multistage multiscale linear stochastic model to optimize electricity generation, storage, and transmission investments over a long planning horizon. The multiscale structure captures ‘large-scale’ uncertainties, such as investment and fuel-cost changes and long-run demand-growth rates, and ‘small-scale’ uncertainties, such as hour-to-hour demand and renewable-availability uncertainty. The model also includes a detailed treatment of operating periods so that the effect of dispatch decisions on long-term investments are captured.

The proposed model can be large in size. The progressive hedging algorithm is applied to decompose the model by scenario, greatly reducing computation times. We also derive bounds on the optimal objective-function value, to assess solution quality. We use a case study based on the state of Texas to demonstrate the model and show the benefits of its detailed representation of the operating periods in making investment decisions.

Index Terms—Power system planning, stochastic optimization, decomposition, progressive hedging algorithm

I. INTRODUCTION

ELECTRICITY demand growth, generator retirements, and technology advances make it necessary to expand generation and transmission capacity. These investments are capital-intensive, time-consuming, and long-lasting. Moreover, generation and transmission investment is subject to considerable short- and long-run uncertainty. Changes in fuel or investment costs can make a seemingly prudent generation technology uneconomic. Uncertain demand-growth rates can affect how much capacity a given system needs. Short-run variability in demand, wind, and solar production can also affect an optimal generation mix.

This paper proposes a centralized planning model to assist a central planner, utility, policy maker, or regulator in optimizing these types of investments. The model is multistage, multiscale, and stochastic, making investment decisions at different points in time with consideration of future uncertainties and investments. The model also includes a detailed representation of operating periods between investments. This allows the effects of short-run uncertainties (*e.g.*, real-time wind, solar, and demand variability) on investments to be captured. The model is multiscale in two senses, which are described further

in Section III, where the model structure and formulation are given. First, we capture different scales of uncertainties that affect planning decisions in different ways. Secondly, we capture decisions that occur on different scales (*i.e.*, relatively coarse time scales for planning decisions, as opposed to fine temporal scales for operating decisions).

With all of these factors being represented, the model can be large in scale and take excessive computation time to be solved. To address the tractability issue, the progressive hedging algorithm (PHA) is implemented to decompose the model per scenario. We demonstrate the use of the model with a case study based on the state of Texas. We compare the solutions obtained from the model using the PHA to those obtained from solving the undecomposed problem (in terms of the objective-function value and investments made). We find that the two sets of investments and their costs are very similar, showing the accuracy of using the PHA to decompose and solve the model. We explore the impact of the penalty coefficient used in the PHA on model performance. We show that using higher coefficient values decreases computation time, with some tradeoff in solution quality. We also show how the detailed representation of the operating periods affects the optimal generation mix.

The remainder of this paper is organized as follows. Section II reviews the existing literature on investment planning and further highlights the contribution of our proposed model. Section III details the structure and mathematical formulation of our model. Section IV discusses the PHA algorithm and how we assess the quality of solutions given by the algorithm. Sections V and VI introduce our case study data and results, respectively. Section VII concludes.

II. LITERATURE REVIEW

Two different approaches are typically applied to power system investment problems: centralized and market-based frameworks [1]. The former considers capacity investment from the perspective of the whole system, typically minimizing cost or maximizing social welfare [2]–[5]. The latter tackles the problem of a market participant, such as a profit-maximizing generating firm [6].

Short *et al.* [3] develop a deterministic cost-minimization model for the deployment of generation technologies and transmission infrastructure throughout the United States, looking forty years into the future. Their work includes a detailed treatment of conventional and renewable generation

This work was supported by NSF grant 1029337.

Y. Liu and R. Sioshansi are with the Department of Integrated Systems Engineering, The Ohio State University, Columbus, OH 43210, USA (e-mail: liu.2441@osu.edu, sioshansi.1@osu.edu).

A. J. Conejo is with the Department of Integrated Systems Engineering and the Department of Electrical and Computer Engineering, The Ohio State University, Columbus, OH 43210, USA (e-mail: conejonavarro.1@osu.edu).

technologies, transmission lines, energy storage, and policy parameters, and has high spatial resolution. On the other hand, their work uses a small set of time slices to represent system-operation costs. Mills and Wiser [4] consider the effect of renewable penetration on investments by using a long-run optimization model that considers both investment and dispatch decisions. Domínguez *et al.* [5] develop a stochastic optimization model to explore how current electric power systems can be transformed into renewable-dominated designs at minimal cost. López *et al.* [2] propose a mixed-integer nonlinear model for generation and transmission expansion that captures risk preferences.

Bilevel approaches are commonly used for modeling investments from the perspective of market participants [6]–[8]. Such approaches allow the representation of a sequential decision-making process in which investments are made before operational decisions. Thus, they are useful when market competition is modeled. This can be contrasted to single-level models, in which all decisions are made simultaneously. Two popular types of bilevel models are mathematical programs with equilibrium constraints and equilibrium problem with equilibrium constraints. The former is suited to modeling capacity expansion decisions made by a single investor, while the latter is suited to modeling multiple firms simultaneously. Wogrin [8] develops bilevel models of generation companies making investment decisions in a highly competitive market. She concludes that models with bilevel structures can provide better results than single-level ones. Chuang *et al.* [9] formulate a generation-expansion problem as a single-level Cournot model. Roh *et al.* [10] propose a stochastic generation and transmission expansion model that considers uncertainties.

Investment planning is usually affected by many factors that are uncertain, such as demand increases, policy changes, and technology advances. Stochastic optimization, as a framework for modeling optimization problems that involve uncertainty, constitutes a useful tool for capturing the impacts of such uncertainties [2], [5]–[8], [10]. A number of works model capacity investment as two-stage or multistage stochastic optimization problems [10]–[17]. However, none of these include the detailed multiscale representation of uncertainties that we propose in our model. Munoz and Watson [18] apply the PHA to a multistage investment model. However, their work does not capture the same level of detail in representing operating decisions that our model does. Instead, they assume that the hourly economic dispatch models are independent and do not capture intertemporal ramping or energy storage-related constraints. Zou *et al.* [19] develop a nested decomposition algorithm, which is similar to the concept of stochastic dual dynamic programming [20], which may prove to be a promising technique to solve multistage stochastic investment models.

Our work makes several contributions to this existing literature on investment planning. Our model optimizes both generation and transmission investment from the perspective of a central planner. The multiscale framework that we adopt allows us to capture both large- and small-scale uncertainties. Moreover, our detailed representation of the operating periods between investment periods allows the effects of intertemporal

constraints, such as generator ramping and energy storage state-of-charge, to be captured in investment decisions. Many existing models use simplified representations of operating periods that are not serially coupled. Our work also proposes the use of PHA as an algorithm to efficiently obtain solutions to the resulting model with bounds on solution quality.

III. CAPACITY-EXPANSION MODEL

Fig. 1 summarizes the overall structure of our proposed capacity-expansion model. The model structure consists of multiple investment periods (denoted by circles in the figure), each of which is followed by a series of operating periods (denoted by squares in the figure). Thus, our model considers an investment stage as consisting of an initial investment decision, followed by operating decisions for the intervening operating periods before the next investment decision is made. The investment and operating decisions are structured in a tree, where the branches correspond to different scenarios of the underlying scenario tree representing uncertainties.

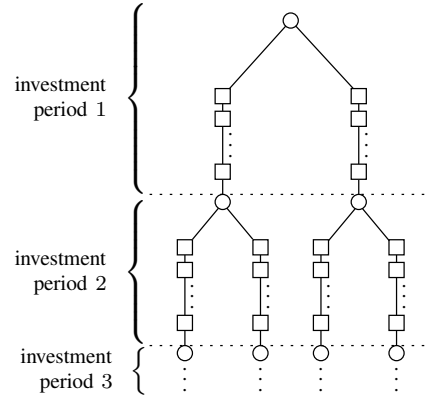


Fig. 1. Structure of capacity-expansion model

Our model is multistage in the sense that investments can be made at multiple points in time (*i.e.*, the circles in Fig. 1). The model is multiscale in terms of how decisions and uncertainties are modeled. Investment decisions are modeled at a relatively coarse time scale (*e.g.*, annually or decennially). Conversely, operating decisions are modeled at a relatively fine time scale (*e.g.*, hourly or subhourly).

Uncertainties are similarly modeled at different scales. The branches of the scenario tree in Fig. 1 capture large-scale uncertainties that occur on similar temporal scales to the investment decisions. Examples of these can include major policy changes (*e.g.*, a carbon tax or renewable portfolio standard), fuel-cost changes, technology development, or long-run demand-growth rates. Finer-scale uncertainties (*e.g.*, seasonal, diurnal, and hourly demand, wind, and solar patterns) are captured through the different deterministic operating periods between investment decisions.

The reason for this disparate representation of large- and small-scale uncertainties is because they affect investment decisions differently. Large-scale uncertainties have a direct and explicit impact on investment decisions. For instance, if prices of some generating fuels may rise or the investment costs of some generation technologies may fall in the future,

such uncertainties should be directly taken into account when making investment decisions. As such, large-scale uncertainties are explicitly represented in the scenario tree. Conversely diurnal or seasonal uncertainty and variability in the real-time availability of renewable generators has a more muted effect on investment decisions. The effect of these uncertainties is primarily on the extent to which flexibility is needed in the power system. Such impacts can be captured in a more implicit manner via different operating periods (which in our work are taken to be representative days modeled at hourly intervals), that represent a wide variety of weather conditions.

In practice, these operating periods may be a weighted subset of hours, days, or weeks chosen by Monte Carlo simulation, importance sampling, clustering, or other techniques. Our model structure is agnostic to the temporal resolution of the operating periods. We assume in our mathematical formulation, however, that the operating periods are representative days of the intervening time between investment periods that are modeled at an hourly time resolution. The use of representative days in modeling the operating periods allows for intertemporal constraints, such as state-of-charge balance for energy storage and generator ramping, to be captured in the model.

A. Model Notation

We begin by defining the following model notation.

1) Sets and Set-Related Parameters:

N	set of generation technologies.
R	set of regions.
T^D	set of operating days between investment periods.
T^H	number of operating hours in each representative day.
T^I	set of investment periods.
Υ^I	number of years between investment periods.
Ω	set of scenarios.
$\bar{\omega}_i$	set of scenarios that are indistinguishable from scenario ω when making investment decisions in investment period i .

2) Parameters:

A_n	lifetime of technology n [investment periods].
$\bar{B}_{n,r,i}$	maximum capacity of technology n that can be built in region r in investment period i [MW].
$C_{\omega,n,r,i}^E$	cost of retiring technology n in region r in investment period i of scenario ω [\$/MW].
$C_{\omega,n,r,i}^G$	generation cost of technology n in region r in investment period i of scenario ω [\$/MWh].
$C_{\omega,r,r'}^L$	investment cost of building transmission between regions r and r' in investment period i of scenario ω [\$/MW].
$C_{\omega,n,r,i,a}^M$	maintenance cost of technology n in region r that is a investment periods old in investment period i of scenario ω [\$/MW].
$C_{\omega,r,i}^S$	investment cost of energy storage in region r in investment period i of scenario ω [\$/MW].
C^U	cost of unserved load [\$/MWh].

$C_{\omega,n,r,i}^V$	investment cost of building technology n in region r in investment period i of scenario ω [\$/MW].
$L_{\omega,r,i,d,h}$	region r 's load in hour h of day d of investment period i of scenario ω [MW].
γ	discount rate.
δ_n	ramping factor of technology n [p.u.].
η	energy capacity of energy storage [hours of storage].
ζ	roundtrip efficiency of energy storage [p.u.].
π_ω	probability of scenario ω .
$\phi_{\omega,n,r,i,d,h}$	capacity factor of technology n in region r in hour h of day d of investment period i of scenario ω [p.u.].
$\Upsilon_{i,d}$	weight on representative day d of investment period i [days].

3) Decision Variables:

$k_{\omega,n,r,i,a}^E$	capacity of technology n in region r with age a that is economically retired in investment period i of scenario ω [MW].
$k_{\omega,n,r,i,a}^G$	total capacity of technology n in region r with age a at the end of investment period i of scenario ω [MW].
$k_{\omega,r,r',i}^L$	capacity added to transmission link between regions r and r' in investment period i of scenario ω [MW].
$k_{\omega,r,i}^S$	capacity of energy storage installed in region r in investment period i of scenario ω [MW].
$K_{\omega,i}$	vector denoting all scenario- ω investment variables (i.e., k 's) of investment period i .
$q_{\omega,r,i,d,h}^C$	hour- h power charged into energy storage in region r on day d of investment period i of scenario ω [MW].
$q_{\omega,r,i,d,h}^D$	hour- h power discharged from energy storage in region r on day d of investment period i of scenario ω [MW].
$q_{\omega,n,r,i,d,h}^G$	hour- h production from technology n in region r on day d of investment period i of scenario ω [MW].
$q_{\omega,r,r',i,d,h}^L$	net power flow on link from region r to r' in hour h of day d of investment period i of scenario ω [MW].
$q_{\omega,r,i,d,h}^S$	hour- h ending state of charge of energy storage in region r on day d of investment period i of scenario ω [MW].
$q_{\omega,r,i,d,h}^U$	hour- h unserved load in region r on day d of investment period i of scenario ω [MW].

B. Model Formulation

Our model is formulated as:

$$\min \sum_{\omega \in \Omega} \pi_\omega \sum_{i \in T^I} \gamma^{i\Upsilon^I} \left\{ \sum_{n \in N, r \in R} \left[C_{\omega,n,r,i}^V k_{\omega,n,r,i,1}^G \right. \right. \quad (1)$$

$$\left. \left. + C_{\omega,n,r,i}^E \cdot \left(k_{\omega,n,r,i,A_n}^G + \sum_{a=1}^{A_n-1} k_{\omega,n,r,i,a}^E \right) \right] \right\}$$

$$\begin{aligned}
& + \sum_{r \in R} C_{\omega,r,i}^S k_{\omega,r,i}^S + \sum_{d \in T^D} \Upsilon_{i,d} \sum_{h=1}^{T^H} C_{\omega,n,r,i}^G q_{\omega,n,r,i,d,h}^G \\
& + \sum_{a=1}^{A_n} C_{\omega,n,r,i,a}^M k_{\omega,n,r,i,a}^G \left. + \sum_{\substack{r,r' \in R \\ r \neq r'}} C_{\omega,r,r'}^L k_{\omega,r,r',i}^L \right\} \\
& + \sum_{r \in R, d \in T^D} \Upsilon_{i,d} \sum_{h=1}^{T^H} C_{\omega,r,i,d,h}^U q_{\omega,r,i,d,h}^U
\end{aligned}$$

$$\text{s.t. } k_{\omega,n,r,i,1}^G \leq \bar{B}_{n,r,i}, \quad \forall \omega, n, r, i \quad (2)$$

$$\begin{aligned}
k_{\omega,n,r,i,a}^G &= k_{\omega,n,r,i-1,a-1}^G - k_{\omega,n,r,i-1,a-1}^E, \quad (3) \\
\forall \omega, n, r, i &\geq 2, a \geq 2
\end{aligned}$$

$$K_{\omega,i} \geq 0, \quad \forall \omega, i \quad (4)$$

$$K_{\omega,i} = K_{\omega',i}, \quad \forall \omega, i, \omega' \in \bar{\omega}_i \quad (5)$$

$$\sum_{n \in N} q_{\omega,n,r,i,d,h}^G + q_{\omega,r,i,d,h}^D - q_{\omega,r,i,d,h}^C + q_{\omega,r,i,d,h}^U \quad (6)$$

$$\begin{aligned}
& + \sum_{\substack{r' \in R \\ r' \neq r}} (q_{\omega,r',i,d,h}^L - q_{\omega,r,r',i,d,h}^L) = L_{\omega,r,i,d,h}, \\
& \forall \omega, n, r, i, d, h
\end{aligned}$$

$$0 \leq q_{\omega,n,r,i,d,h}^G \leq \phi_{\omega,n,r,i,d,h} \sum_{a=1}^{A_n} k_{\omega,n,r,i,a}^G, \quad (7)$$

$$\forall \omega, n, r, i, d, h$$

$$-\delta_n \sum_{a=1}^{A_n} k_{\omega,n,r,i,a}^G \leq q_{\omega,n,r,i,d,h}^G - q_{\omega,n,r,i,d,h-1}^G \quad (8)$$

$$\leq \delta_n \sum_{a=1}^{A_n} k_{\omega,n,r,i,a}^G, \quad \forall \omega, n, r, i, d, h$$

$$-\sum_{i' \leq i} k_{\omega,r,r',i'}^L \leq q_{\omega,r,r',i,d,h}^L \leq \sum_{i' \leq i} k_{\omega,r,r',i'}^L, \quad (9)$$

$$\forall \omega, r, r' \neq r, i, d, h$$

$$\begin{aligned}
q_{\omega,r,i,d,h}^S &= q_{\omega,r,i,d,h-1}^S - q_{\omega,r,i,d,h}^D + \zeta q_{\omega,r,i,d,h}^C, \quad (10) \\
\forall \omega, r, i, d, h &\geq 2
\end{aligned}$$

$$q_{\omega,r,i,d,0}^S = \frac{1}{2} \eta \sum_{i' \leq i} k_{\omega,r,i'}^S, \quad \forall \omega, r, i, d \quad (11)$$

$$q_{\omega,r,i,d,T^H}^S = \frac{1}{2} \eta \sum_{i' \leq i} k_{\omega,r,i'}^S, \quad \forall \omega, r, i, d \quad (12)$$

$$0 \leq q_{\omega,r,i,d,h}^S \leq \eta \sum_{i' \leq i} k_{\omega,r,i'}^S, \quad \forall \omega, r, i, d, h \quad (13)$$

$$0 \leq q_{\omega,r,i,d,h}^C, q_{\omega,r,i,d,h}^D \leq \sum_{i' \leq i} k_{\omega,r,i'}^S, \quad (14)$$

$$\forall \omega, r, i, d, h$$

$$0 \leq q_{\omega,r,i,d,h}^U \leq L_{\omega,r,i,d,h}, \quad \forall \omega, n, r, i, d, h. \quad (15)$$

Objective function (1) minimizes expected discounted cost over the planning horizon. The objective function includes seven cost components. The first, $C_{\omega,n,r,i}^V k_{\omega,n,r,i,1}^G$, is the cost of investing in new generating capacity. New generating capacity that is added in investment period i is, by definition, $a = 1$ investment periods old at the end of investment period i , which is why new capacity is given by $k_{\omega,n,r,i,1}^G$.

The second is the cost of retiring generating capacity (*e.g.*, cleanup and reactor dismantling for a nuclear unit). The model allows for two types of retirements. The first is due to age, once a technology has reached its fixed operating life. Technology n is assumed to have an operating life of A_n investment periods. The other is economic retirement, meaning that the model chooses to retire a technology before its operating life, for instance due to changes in operating and maintenance costs of one technology relative to another.

The third is the cost of adding energy storage to the system. The fourth is generator operating costs. Operating costs for each hour of each representative day are added together and multiplied by $\Upsilon_{i,d}$, which is the weight placed on each operating day. The fifth cost is generator maintenance costs, which are allowed to vary with age. This can represent technologies becoming more costly to maintain as they age. The sixth is the cost of adding capacity to transmission links between the regions of the power system modeled. We use a pipeline model of the transmission system, as opposed to a load-flow model. The seventh is the cost of unserved load, which may occur if available generating capacity is insufficient (or insufficiently flexible) to meet load in a particular operating period.

We use a pipeline model of the transmission system because a load-flow model would require the use of binary variables to represent transmission investments. Transmission investments with a load-flow model must be represented as being ‘lumpy,’ because adding new transmission lines impacts transmission flows on other elements in the network. Using a pipeline model does not provide a perfect representation of load flows. However, Ahlhaus and Stursberg [21] suggest a method of modeling transmission investments using a pipeline model that provides precision that is comparable to a load-flow model. Thus, our model can be easily extended using their method, which would yield improved accuracy at a reduced computational cost (compared to employing a load-flow model).

Objective function (1) could also include other costs that we do not model. As an example, energy storage and transmission could have retirement, maintenance, and operating costs. Storage operating costs could be a means of more accurately capturing hybrid technologies, such as diabatic compressed air energy storage, which require an input fuel [22]. Our analysis focuses on bulk energy storage technologies, such as pumped hydroelectric storage, which is not a hybrid technology.

The model has two types of constraints. Constraints (2)–(5) pertain to the investment whereas constraints (6)–(15) pertain to the operating periods. Constraints (2) imposes limits on generation technology investments, for instance due to land restrictions, resource availability, or policy restrictions. Constraints (3) define the amount of generating capacity of different ages in each investment period as the previous amount of capacity less retirements. Constraints (4) impose non-negativity on the investment variables. Constraints (5) are the non-anticipativity constraints, which impose the structure of the scenario tree on the decisions. This is done by ensuring that decisions made in each investment period are not dependent on future scenario realizations. For instance, in the scenario-tree depicted in Fig. 1, the period-1 investment decisions would

have to be the same across all of the scenarios. However, the period-2 investments of the scenarios emanating from the left-hand side of the scenario tree could be different from those of the scenarios emanating from the right-hand side of the tree.

Constraints (6) impose load-balance in each operating period. Constraints (7) and (8) impose capacity and ramping limits on generators. The capacity limits are defined based on total installed capacity available multiplied by a capacity factor. The capacity factor can capture hour-to-hour variability in wind, solar, and other renewable availability. The ramping limit is assumed to be a multiple of the installed capacity, with higher values of δ_n denoting a more flexible generating technology. Constraints (9) impose transmission-capacity limits.

Constraints (10)–(14) pertain to the operation of energy storage. Constraints (10) define the ending state of charge of storage in each hour. Constraints (11) and (12) force each storage device to begin and end each day with a 50% state of charge. This is a heuristic technique to attach carryover value to stored energy from one day to the next [23]. Constraints (13) and (14) impose energy and power limits on storage. The energy capacity of storage is measured by the number of hours of full power output [24].

Constraints (10)–(14) do not account for cycle-life degradation of energy storage, which may be an important consideration for some technologies. One could modify the energy or power capacities of the storage device to include a linear degradation term that depends on total aggregate MWh of energy that has been ‘cycled’ through the storage technology in previous operating periods [25].

Constraints (15) limit the amount of unserved energy in each operating period to be no greater than demand. Explicit non-anticipativity constraints on the operating decisions are not needed, as non-anticipativity constraints on the investment decisions will enforce non-anticipativity of the operating decisions.

IV. PROGRESSIVE HEDGING ALGORITHM

Depending on the number of investment and operating periods and scenarios included in it, our proposed capacity-expansion model can be large in scale and computationally intractable. We apply the PHA [26], which is an augmented Lagrangian method, to decompose the problem per scenario by relaxing non-anticipativity constraints (5) and penalizing constraint violations in the objective function.

PHA can be used to obtain a feasible solution to the original problem, which also provides an upper bound on the optimal objective-function value. Gade *et al.* [27] derive a lower bound on the optimal objective-function value for a two-stage mixed-integer stochastic optimization problem. We extend their proof to a multistage stochastic problem, allowing us to assess the quality of solutions generated by the PHA.

We first outline the PHA for a general multistage stochastic optimization problem in Section IV-A. We then give the lower-bound result in Section IV-B.

A. Progressive Hedging Algorithm for Multistage Stochastic Optimization Problems

We begin by giving the following generic scenario-based formulation of a multistage stochastic optimization problem. To do so we first define the following additional notation (sets, parameters, and variables that are not defined have the same definitions as in Section III-A):

I number of stages.

$x_{\omega,i}$ stage- i decision of scenario ω .

A generic multistage stochastic optimization problem can then be formulated as:

$$\min_x \sum_{\omega \in \Omega} \pi_{\omega} \sum_{i=1}^I \psi_{\omega,i}^{\top} x_{\omega,i} \quad (16)$$

$$\text{s.t. } M_{\omega,1} x_{\omega,1} = \kappa_{\omega,1}, \quad \forall \omega \in \Omega \quad (17)$$

$$M_{\omega,i} x_{\omega,i} = \kappa_{\omega,i} - \mu_{\omega,i} x_{\omega,i-1}, \quad (18)$$

$$\forall \omega \in \Omega, i = 2, \dots, I$$

$$x_{\omega,i} \geq 0, \quad \forall \omega \in \Omega, i = 1, \dots, I \quad (19)$$

$$x_{\omega,i} = x_{\omega',i}, \quad \forall \omega \in \Omega, i = 1, \dots, I, \omega' \in \bar{\omega}_i. \quad (20)$$

Objective function (16) minimizes expected cost, with $\psi_{\omega,i}$ denoting stage- i cost coefficients under scenario ω . Constraints (17) and (18) impose structural constraints on the decisions with $M_{\omega,i}$, $\kappa_{\omega,i}$, and $\mu_{\omega,i}$ being matrices of coefficients and vectors of constants of appropriate dimensions. Constraints (19) and (20), respectively, impose non-negativity and non-anticipativity.

To outline the PHA, we next define for each scenario, $\omega \in \Omega$:

$$X_{\omega} = \{x_i, i = 1, \dots, I \mid M_{\omega,1} x_{\omega,1} = \kappa_{\omega,1}, \\ M_{\omega,i} x_{\omega,i} = \kappa_{\omega,i} - \mu_{\omega,i} x_{\omega,i-1}, x_{\omega,i} \geq 0\}, \quad (21)$$

as the scenario- ω feasible set. PHA decomposes problem (16)–(20) by dualizing non-anticipativity constraints (20).

To give the relaxed problem, we first define $\lambda_{\omega,i}^v$ as the Lagrange-multiplier vector associated with the non-anticipativity constraint on $x_{\omega,i}$. The superscript, v , on the multiplier vector corresponds to the iteration counter of the PHA. We also define:

$$\hat{x}_{\omega,i}^v = \frac{\sum_{\omega' \in \bar{\omega}_i} \pi_{\omega'} x_{\omega',i}^v}{\sum_{\omega' \in \bar{\omega}_i} \pi_{\omega'}}, \quad (22)$$

where $x_{\omega',i}^v$ is the value of $x_{\omega',i}$ in the v th iteration of the PHA, as the probability-weighted average of the $x_{\omega',i}$'s that should be equal to $x_{\omega,i}$ per non-anticipativity constraints (20). The v superscript on $\hat{x}_{\omega,i}^v$ denotes that this is the value of the average in the v th iteration of the PHA. The relaxed problem is given by:

$$\min_x \sum_{\omega \in \Omega} \pi_{\omega} \sum_{i=1}^I \left(\psi_{\omega,i}^{\top} x_{\omega,i} + \lambda_{\omega,i}^{v \top} x_{\omega,i} \right. \quad (23)$$

$$\left. + \frac{\rho}{2} \|x_{\omega,i} - \hat{x}_{\omega,i}^v\|^2 \right)$$

$$\text{s.t. } x_{\omega,i} \in X_{\omega}, \quad \forall \omega \in \Omega, i = 1, \dots, I. \quad (24)$$

Objective function (23) includes two penalty terms. The first, $\lambda_{\omega,i}^v \top x_{\omega,i}$, is a standard Lagrange-multiplier term. The other penalizes the value of $x_{\omega,i}$ deviating from $\hat{x}_{\omega,i}^v$. The coefficient $\rho > 0$ determines how much to penalize the deviation of the scenario solution from this average.

Algorithm 1 outlines the steps of the PHA. The penalty coefficient and convergence tolerance are input in step 1. Step 2 initializes the iteration counter and Lagrange-multiplier vectors. In Steps 3–5 each scenario subproblem is solved without the penalty terms (*i.e.*, minimizing objective function (16) of the original problem). These starting values of $x_{\omega,i}$ are used to initialize the Lagrange-multiplier vectors in Steps 7 and 8 by first updating \hat{x}_i and then the multiplier vectors themselves.

Algorithm 1 Progressive Hedging Algorithm

- 1: **input:** ρ, ϵ
 - 2: **initialization:** $v \leftarrow 0, \lambda_{\omega,i}^v \leftarrow 0 \forall \omega \in \Omega, i = 1, \dots, I$
 - 3: **for** $\omega \in \Omega$ **do**
 - 4: $x_{\omega,i}^v \leftarrow \arg \min_x (16)$ s.t. (24)
 - 5: **end for**
 - 6: **repeat**
 - 7: $\hat{x}_i^v \leftarrow \sum_{\omega' \in \bar{\omega}_i} \pi_{\omega'} x_{\omega',i}^v / \sum_{\omega' \in \bar{\omega}_i} \pi_{\omega'} \forall i = 1, \dots, I$
 - 8: $\lambda_{\omega,i}^{v+1} \leftarrow \lambda_{\omega,i}^v + \rho \cdot (x_{\omega,i}^v - \hat{x}_{\omega,i}^v) \forall \omega \in \Omega, i = 1, \dots, I$
 - 9: $v \leftarrow v + 1$
 - 10: $x_{\omega,i}^v \leftarrow \arg \min_x (23)$ s.t. (24)
 - 11: **until** $\|x_{\omega,i}^v - \hat{x}_{\omega,i}^v\| < \epsilon \forall \omega \in \Omega, i = 1, \dots, I$
-

Steps 6–11 are the main iterative loop. Steps 7 and 8 update the Lagrange multipliers based on the most recent values of $x_{\omega,i}$. Step 9 updates the iteration counter, and Step 10 resolves the relaxed problem with the updated multipliers. This loop repeats until each non-anticipativity constraint is satisfied within the specified convergence tolerance.

B. Lower Bound for Progressive Hedging Algorithm

We can derive a lower bound on the optimal objective-function value of a multistage stochastic optimization problem solved using PHA from the Lagrange multipliers on the non-anticipativity constraints. To do so, we let z^* denote the optimal objective-function value of problem (16)–(20) and let $x_{\omega,i}^*$ denote a corresponding set of optimal decision policies. We assume that problem (16)–(20) is bounded and feasible. Thus, we have that $-\infty < z^* < +\infty$ and $x_{\omega,i}^* \in X_{\omega} \neq \emptyset, \forall \omega \in \Omega$.

We first prove the following lemma.

Lemma 1: In each iteration of Algorithm 1, the following condition holds:

$$\sum_{\omega \in \Omega} \pi_{\omega} \sum_{i=1}^I \lambda_{\omega,i}^v \top x_{\omega,i}^* = 0. \quad (25)$$

Proof: We can show this by induction. For $v = 0$ we have $\lambda_{\omega,i}^1 = \rho \cdot (x_{\omega,i}^0 - \hat{x}_{\omega,i}^0)$. Thus, $\forall \omega \in \Omega, i = 1, \dots, I$, we

have that:

$$\sum_{\omega \in \Omega} \pi_{\omega} \lambda_{\omega,i}^1 = \rho \sum_{\omega \in \Omega} \pi_{\omega} \cdot (x_{\omega,i}^0 - \hat{x}_{\omega,i}^0) \quad (26)$$

$$= \rho \sum_{\omega \in \Omega} \pi_{\omega} \frac{\sum_{\omega' \in \bar{\omega}_i} \pi_{\omega'} \cdot (x_{\omega,i}^0 - x_{\omega',i}^0)}{\sum_{\omega' \in \bar{\omega}_i} \pi_{\omega'}} \quad (27)$$

$$= 0. \quad (28)$$

By induction on the Lagrange-multiplier update in Step 8 of Algorithm 1 we can show that (25) holds for all remaining iterations of the PHA. This is because the best possible lower bound obtained using dual prices is as tight as the lower bound obtained using the dual decomposition method [27]. ■

We next define:

$$\xi_{\omega}(\lambda_{\omega}^v) = \min_{x \in X_{\omega}, \forall \omega \in \Omega} \left\{ \sum_{i=1}^I \left(\psi_{\omega,i}^{\top} x_{\omega,i} + \lambda_{\omega,i}^v \top x_{\omega,i} \right) \right\}, \quad (29)$$

and:

$$\Xi(\lambda^v) = \sum_{\omega \in \Omega} \pi_{\omega} \xi_{\omega}(\lambda_{\omega}^v), \quad (30)$$

and prove the following theorem establishing the bound.

Theorem 1: $\Xi(\lambda^v) \leq z^*, \forall v$.

Proof: From the definition of $\xi_{\omega}(\lambda_{\omega}^v)$ and $x_{\omega,i}^*$ we have:

$$\xi_{\omega}(\lambda_{\omega}^v) \leq \sum_{i=1}^I \left(\psi_{\omega,i}^{\top} x_{\omega,i}^* + \lambda_{\omega,i}^v \top x_{\omega,i}^* \right). \quad (31)$$

Combining this with the definition of $\Xi(\lambda)$ and Lemma 1 we then have:

$$\Xi(\lambda^v) = \sum_{\omega \in \Omega} \pi_{\omega} \xi_{\omega}(\lambda_{\omega}^v) \quad (32)$$

$$\leq \sum_{\omega \in \Omega} \pi_{\omega} \sum_{i=1}^I \left(\psi_{\omega,i}^{\top} x_{\omega,i}^* + \lambda_{\omega,i}^v \top x_{\omega,i}^* \right) \quad (33)$$

$$= \sum_{\omega \in \Omega} \pi_{\omega} \sum_{i=1}^I \psi_{\omega,i}^{\top} x_{\omega,i}^* \quad (34)$$

$$+ \sum_{\omega \in \Omega} \pi_{\omega} \sum_{i=1}^I \lambda_{\omega,i}^v \top x_{\omega,i}^*$$

$$= \sum_{\omega \in \Omega} \pi_{\omega} \sum_{i=1}^I \psi_{\omega,i}^{\top} x_{\omega,i}^* \quad (35)$$

$$= z^*, \quad (36)$$

proving the result. ■

V. CASE STUDY DATA

We apply our proposed capacity-expansion model to a numerical case study based on the state of Texas [28]. The state is modeled as consisting of three regions (west, east, and south Texas) that are connected by three transmission corridors. The case study begins in the year 2010 and the model has between four and six investment periods that occur at ten-year intervals (*i.e.*, we conduct a sensitivity analysis in which the number of investment periods is changed).

We model five generic generation technologies: wind, solar, nuclear-powered, and natural gas- and coal-fired units. A generic energy storage technology is also modeled. The ‘large-scale’ uncertainties, which are explicitly modeled in the scenario tree, are changes in investment costs and generating-fuel prices. Scenarios around these parameters are generated from values reported in the United States Energy Information Administration’s 2014 Annual Energy Outlook [29] and other sources [30].

Table I summarizes the ranges of percentage decreases (relative to the 2010 levels) in wind and solar investment costs represented in the scenarios. These cost decreases mostly represent the effects of technology improvement. Table II summarizes the ranges of percentage increases (relative to the 2010 levels) in operating costs of coal- and natural gas-fired generators. These scenarios reflect the impacts of changing fuel supply and demand and can also capture policy impacts (*e.g.*, carbon policies on operating costs of fossil fuels).

TABLE I
RANGE OF INVESTMENT-COST DECREASES [% RELATIVE TO 2010 LEVELS] IN DIFFERENT SCENARIOS

Technology	Year		
	2020	2030	2040
Wind	5–10	10–20	15–30
Solar	5–10	10–20	15–30

TABLE II
RANGE OF OPERATING-COST INCREASES [% RELATIVE TO 2010 LEVELS] IN DIFFERENT SCENARIOS

Technology	Year		
	2020	2030	2040
Coal	0–3	1–7	3–28
Natural Gas	0–5	1–18	3–54

The base case, in which there are four investment periods, has a scenario tree with $2^7 = 128$ scenarios. Retirement and maintenance costs, ramping capabilities, and technology lifetimes are obtained from the same sources as the other cost data. Renewable resource limits, for instance associated with land use, are obtained from Lopez *et al.* [31]. We assume no resource limits on other technologies.

The operating periods between successive investment periods consist of 30 representative days that are selected from the 10 intervening years using a hierarchical clustering technique [28]. The clustering technique also provides the weights for each modeled day. Our numerical testing indicates that 30 representative days provides a sufficiently rich set of operating conditions to represent demand, wind, and solar conditions well and provide investment decisions that are very similar to using the full set of operating days [28]. Conversely, using fewer representative operating days may result in solutions that give a similar objective-function value to using the full set of operating days, but vastly different investment levels.

Weather conditions, which drive solar and wind availability and demand patterns, are simulated using a time series approach [32]. Electricity-demand patterns are modeled using

Monte Carlo simulation [33] and time series techniques [34]. We assume a 7% discount rate and a load-curtailment cost of \$5000/MWh. The model is implemented in Java and solved using `cplex` version 12.6 on a system with a 3.10 GHz Intel Core i7-3770S processor and 8 GB of memory.

VI. CASE STUDY RESULTS

We conduct four analyses with our case study. First we compare the solutions obtained from and the computation times of solving the full undecomposed capacity-expansion model and the model decomposed using PHA. Next we examine the convergence of the PHA and the role of the penalty parameter (*i.e.*, the value of ρ) in computation time and solution quality. Third we examine how model size affects solution times. Finally, we examine how the inclusion of generator ramping constraints in the operating periods affects optimal investment decisions.

A. Solution Time and Quality of Progressive Hedging Algorithm

Table III summarizes the performance of the PHA in solving instances of the capacity-expansion model with four investment periods and with either one or three representative operating days between successive investment periods. A termination criterion of $\epsilon = 10000$ is used in the PHA. This performance is compared to solving the full undecomposed model. We solve instances with one or three operating days because larger instances of the undecomposed problem cannot be solved directly using `cplex`.

TABLE III
PERFORMANCE OF PROGRESSIVE HEDGING ALGORITHM WITH DIFFERENT NUMBER OF DAYS IN OPERATING STAGE

	Number of Operating Days	
	1	3
Number of Variables	511 488	1 396 224
Number of Constraints	809 002	2 301 994
Undecomposed Problem		
CPU Time [s]	370	17 503
Objective [\$ billion]	554.34	761.77
Decomposed Problem		
CPU Time [s]	271	3 026
Upper Bound [\$ billion]	557.39	762.56
Lower Bound [\$ billion]	551.99	760.27
Optimality Gap [%]	0.97	0.30

The numbers of variables and constraints nearly triple if there are three operating days (relative to one day). With one day, the model is relatively small and the undecomposed model can be easily solved. Thus, decomposing this model using PHA does not afford much benefit in terms of computation time. However, with three operating days, applying PHA reduces the computation time by close to 96% while obtaining a 0.3% optimality gap on the objective-function value.

Figs. 2 and 3 summarize the optimal investments determined by the full and decomposed model in the most likely scenario of the scenario tree. The investment decisions given by the solutions are very similar. The maximum absolute differences in total investment capacities of the different technologies between the two sets of solutions is 12% and 6% with one and

three operating days being modeled, respectively. Moreover, there is a less than 1% difference in total capacity (of all technologies) added between the two sets of solutions. More capacity is built when three operating days are modeled, because the operating days capture more load, wind, and solar variability than one day does.

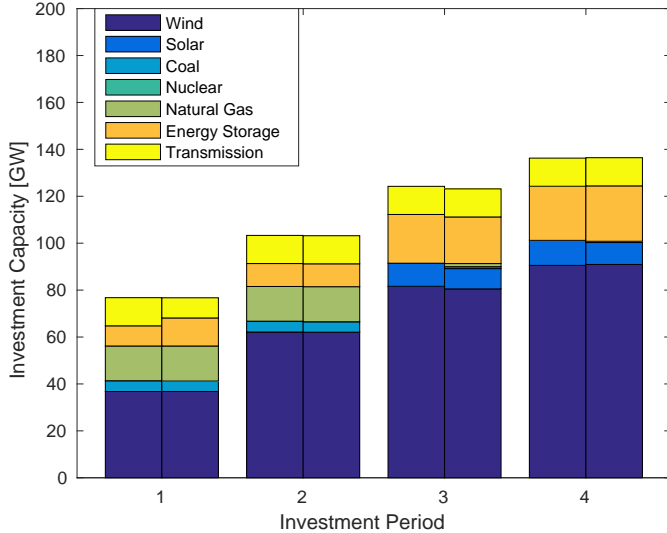


Fig. 2. Optimal investments from solving the full and decomposed model in most likely scenario with one representative operating day between successive investment periods. The left-hand bar (from each pair) shows investments from solving the full model.

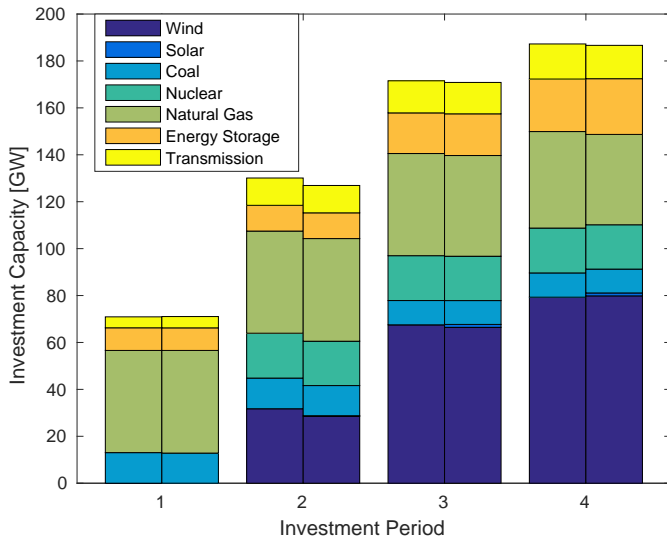


Fig. 3. Optimal investments from solving the full and decomposed model in most likely scenario with three representative operating days between successive investment periods. The left-hand bar (from each pair) shows investments from solving the full model.

Figs. 2 and 3 contrast investment levels obtained from using the PHA to those given by solving the full undecomposed model. These figures *do not* compare investment levels when using a subset of representative operating days to the investment levels obtained when modeling the full set of days. Our numerical testing [28] suggests that about 30 representative operating days is needed to obtain investment levels that are

similar to those given by a model that uses all 365 days of the year. Using three representative operating days can result in investment levels that are, on average, 65% different from the investment levels given by the full set of operating days.

B. Sensitivity of Progressive Hedging Algorithm to ρ

Large values of ρ accelerate the convergence of PHA while smaller values tend to improve the quality of the solution found [35]. To investigate the impact of ρ on PHA solutions, a four-stage model with three operating days between successive investment periods is solved. Four different values of ρ are tested with the same termination criteria of $\epsilon = 10000$. Table IV summarizes the corresponding computation times and solution quality. As the value of ρ increases, fewer iterations and less time are required to achieve the termination criteria. However, these time savings come with a larger final optimality gap. The number of iterations and computation time nearly double when a value of $\rho = 2000$ is compared to $\rho = 100$. In all four cases, the average time per iteration is roughly the same.

TABLE IV
COMPUTATION TIME AND SOLUTION QUALITY OF PROGRESSIVE HEDGING ALGORITHM WITH DIFFERENT VALUES OF ρ

ρ	CPU Time [s]	Number of Iterations	Objective-Function Bound [\$ billion]		Optimality Gap [%]
			Upper	Lower	
100	3 262	38	761.83	761.68	0.02
500	2 167	26	762.07	761.33	0.10
1 000	1 798	23	762.56	760.20	0.31
2 000	1 564	19	763.30	755.63	1.02

Fig. 4 shows the convergence of the upper and lower bounds throughout the iterations of the PHA with different values of ρ . This figure shows the progress beginning from iteration 10, because the bounds make the scales of the vertical axis extremely large if the figure begins from the first iteration. The figure shows that larger values of ρ results in the PHA converging faster (*i.e.*, the algorithm terminates after fewer iterations). However, the lower bounds and optimality gaps tend to be worse with higher values of ρ .

C. Model Size

We next examine the effect of changing the size of the capacity-expansion model, by increasing the number of investment periods, on the performance of the PHA. Table V summarizes the size of models (*i.e.*, number of scenarios, variables, and constraints) with four, five, and six investment periods and 30 representative operating days giving the operating periods between successive investment periods. The table also summarizes the computation time and quality of the solution found by the PHA.

All three cases involve solving massive models with millions of variables and constraints. The solution times in the three cases are around six hours, three days, and more than one week, respectively. Although these solution times are quite long, they are reasonable for an investment model, which may only need to be solved a handful of times to determine investments on an annual basis.

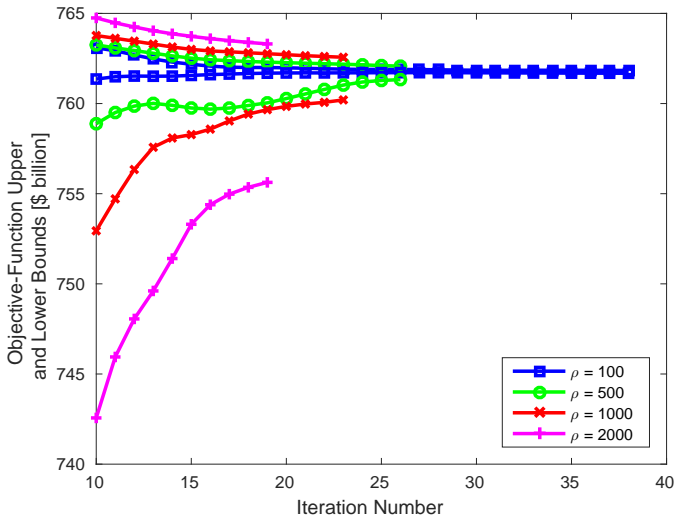


Fig. 4. Objective-function upper and lower bounds throughout iterations of the progressive hedging algorithm with different values of ρ .

TABLE V
COMPUTATION TIME AND SOLUTION QUALITY OF PROGRESSIVE HEDGING ALGORITHM WITH DIFFERENT NUMBER OF INVESTMENT PERIODS

	Number of Investment Periods		
	4	5	6
Number of Scenarios	128	512	2048
Number of Variables [million]	13.34	66.70	320.16
Number of Constraints [million]	22.45	112.28	538.97
CPU Time [s]	21 901	291 139	1 236 442
Number of PHA Iterations	15	26	19
Upper Bound [\$ billion]	758.45	883.76	1 004.89
Lower Bound [\$ billion]	757.60	878.02	992.44
Optimality Gap [%]	0.1	0.6	1.2

Fig. 5 summarizes the optimal investments in the most likely scenario of the scenario tree with four investment periods. Wind and solar are added to the system in later periods when their investment costs become low relative to conventional technologies. The model also opts to economically retire about 3.8 GW of natural gas-fired generation (representing about 10% of installed capacity) in the final investment period before the lifetime of the plants is reached. This is done because lower-cost wind and solar are able to replace the natural gas-fired generation.

D. Effect of Generator Ramping Constraints

Our final analysis examines the effect of having generator ramping constraints in the operating periods on investment decisions. The inclusion of ramping constraints is allowed by us using representative days (as opposed to hours or time slices) in the operating periods of the capacity-expansion model. Fig. 6 summarizes the optimal investments in the most likely scenario of the scenario tree with four investment periods and the generator ramping constraints relaxed in the operating periods of 30 representative days. Contrasting this with Fig. 5 shows that the model builds considerably more nuclear-powered and less natural gas-fired, wind, and solar generation if ramping constraints are ignored. This is because nuclear has a relatively low operating cost and if ramping

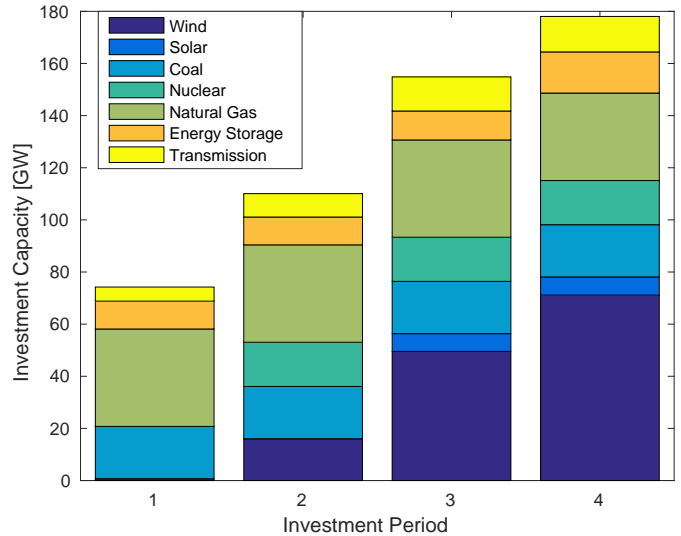


Fig. 5. Optimal investments in most likely scenario with four investment periods and 30 representative operating days between successive investment periods.

constraints are neglected its operational inflexibility does not limit its use to handle ramps in the net load profile. Indeed, without ramping constraints the model economically retires about 20 GW of natural gas-fired capacity in investment periods 2–4, as more nuclear capacity is built. The model also builds less energy storage without ramping constraints. Finally, we note that total installed capacity is lower if ramping constraints are neglected. This means that about 30% of the capacity that the model builds is needed to provide sufficient ramping capability to the system.

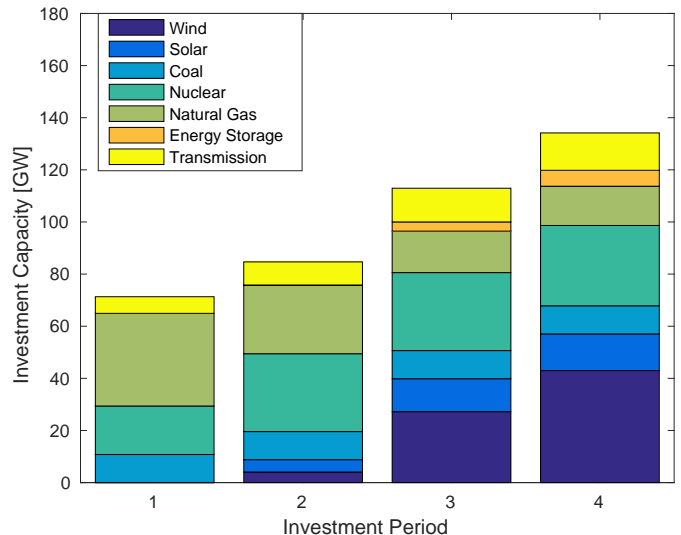


Fig. 6. Optimal investments in most likely scenario with four investment periods, 30 representative operating days between successive investment periods, and ramping constraints relaxed in operating periods.

VII. CONCLUSIONS

This paper presents a multistage, multiscale stochastic investment planning model to assist generators, regulators,

policy makers, and others to plan and study power system investments over the long run. Large-scale uncertainties, such as cost changes and demand-growth rates, are captured explicitly through a scenario tree. Fine-scale demand, wind, and solar variability are represented via different deterministic representative days in the operating periods between successive investment periods. The use of operating days allows important intertemporal constraints, such as energy storage state-of-charge-balance and generator ramping, to be modeled.

Our multiscale approach to representing decisions and uncertainties allows us to capture many operating and investment periods. For instance, the model developed by Short *et al.* [3] represents operations between successive investment epochs using 17 timeslices. Our model, conversely, represents operations using $30 \times 24 = 720$ representative operating hours between investment periods. Indeed, our model and the PHA are capable of tractably including more than 30 representative operating days between investment periods. However, our numerical testing suggests that 30 days provides sufficient granularity around small-scale uncertainties for the purposes of investment planning [28].

The other benefit of our multiscale representation is that it allows us to capture both large- and small-scale uncertainties. Most other works use a relatively coarse representation of *all* uncertainties, meaning that they do not achieve the same fidelity that our model does. On the other hand, a model that fully represents all uncertainties on the same fine scale would be computationally intractable. Thus, our approach provides a good balance between model fidelity and tractability.

The resulting model is large and can be effectively solved using the PHA. The PHA decomposes the problem by scenario and solves each scenario problem, making the problem tractable. The existence of a lower bound for the PHA is shown, allowing solution quality to be assessed.

The performances of the model and PHA are demonstrated through a numerical case study. We find that the decomposed model chooses investments that very closely match those given by the full model. We also investigate the importance of the ρ parameter in the performance of the PHA. Larger values considerably reduce solution times, but at the cost of larger optimality gaps. We explore the effects of increasing the size of the investment model and scenario tree. Problems with hundreds of millions of variables and constraints can be effectively solved using the PHA. We also conduct other numerical testing (beyond that presented in this paper) to examine the effects of other parameters on the performance of the model and PHA [28]. This includes analyses of different load, wind, and solar profiles (corresponding to other geographic regions outside Texas) and different operating and investment costs. The model and PHA show the same performance in these cases as those summarized in Section VI for the case study presented in this paper. We do not include the results of these cases, for reasons of brevity, and instead refer interested readers to the work of Liu [28] for further details.

Our multiscale modeling approach and use of the PHA allow us to solve models that are substantively different in their level of detail in representing decisions and uncertainties compared to other works in the literature [2], [5], [12]–[18].

Thus, our model cannot be directly compared to these works because of the different focus in model detail.

ACKNOWLEDGMENT

Thank you to Armin Sorooshian, the editors, and four anonymous reviewers for helpful suggestions, comments, and conversations.

REFERENCES

- [1] R. M. Kovacevic, G. C. Pflug, and M. T. Vespucci, Eds., *Handbook of Risk Management in Energy Production and Trading*, ser. International Series in Operations Research & Management Science. New York, New York: Springer Science+Business Media, LLC, 2013, vol. 199.
- [2] J. Álvarez López, K. Ponnambalam, and V. H. Quintana, "Generation and Transmission Expansion Under Risk Using Stochastic Programming," *IEEE Transactions on Power Systems*, vol. 22, pp. 1369–1378, August 2007.
- [3] W. Short, P. Sullivan, T. Mai, M. Mowers, C. Uriarte, N. Blair, D. Heimiller, and A. Martinez, "Regional Energy Deployment System (ReEDS)," National Renewable Energy Laboratory, Tech. Rep. NREL/TP-6A20-46534, December 2011.
- [4] A. Mills and R. Wiser, "Changes in the Economic Value of Variable Generation at High Penetration Levels: A Pilot Case Study of California," Ernest Orlando Lawrence Berkeley National Laboratory, Tech. Rep. LBNL-5445E, June 2012.
- [5] R. Domínguez, A. J. Conejo, and M. Carrión, "Toward Fully Renewable Electric Energy Systems," *IEEE Transactions on Power Systems*, vol. 30, pp. 316–326, January 2015.
- [6] S. J. Kazempour, "Strategic Generation Investment and Equilibria in Oligopolistic Electricity Markets," Ph.D. dissertation, Universidad de Castilla-La Mancha, Ciudad Real, Spain, May 2013.
- [7] L. Baringo, "Stochastic Complementarity Models for Investment in Wind-Power and Transmission Facilities," Ph.D. dissertation, Universidad de Castilla-La Mancha, Ciudad Real, Spain, October 2013.
- [8] S. Wogrin, "Generation Expansion Planning in Electricity Markets with Bilevel Mathematical Programming Techniques," Ph.D. dissertation, Universidad Pontificia Comillas, Madrid, Spain, June 2013.
- [9] A. S. Chuang, F. Wu, and P. Varaiya, "A Game-Theoretic Model for Generation Expansion Planning: Problem Formulation and Numerical Comparisons," *IEEE Transactions on Power Systems*, vol. 16, pp. 885–891, November 2001.
- [10] J. H. Roh, M. Shahidehpour, and L. Wu, "Market-Based Generation and Transmission Planning With Uncertainties," *IEEE Transactions on Power Systems*, vol. 24, pp. 1587–1598, August 2009.
- [11] S. Wogrin, E. Centeno, and J. Barquin, "Generation Capacity Expansion in Liberalized Electricity Markets: A Stochastic MPEC Approach," *IEEE Transactions on Power Systems*, vol. 26, pp. 2526–2532, November 2011.
- [12] A. Khodaei, M. Shahidehpour, L. Wu, and Z. Li, "Coordination of Short-Term Operation Constraints in Multi-Area Expansion Planning," *IEEE Transactions on Power Systems*, vol. 27, pp. 2242–2250, November 2012.
- [13] D. Mejía-Giraldo and J. D. McCalley, "Maximizing Future Flexibility in Electric Generation Portfolios," *IEEE Transactions on Power Systems*, vol. 29, pp. 279–288, January 2014.
- [14] S. Jin, A. Botterud, and S. M. Ryan, "Temporal Versus Stochastic Granularity in Thermal Generation Capacity Planning With Wind Power," *IEEE Transactions on Power Systems*, vol. 29, pp. 2033–2041, September 2014.
- [15] L. Tang and M. C. Ferris, "A Hierarchical Framework for Long-Term Power Planning Models," *IEEE Transactions on Power Systems*, vol. 30, pp. 46–56, January 2015.
- [16] I. Konstantelos and G. Strbac, "Valuation of Flexible Transmission Investment Options Under Uncertainty," *IEEE Transactions on Power Systems*, vol. 30, pp. 1047–1055, March 2015.
- [17] H. Ergun, B. Rawn, R. Belmans, and D. Van Hertem, "Stepwise Investment Plan Optimization for Large Scale and Multi-Zonal Transmission System Expansion," in *Power Engineering Society General Meeting*. Boston, MA, USA: Institute of Electrical and Electronics Engineers, 17–21 July 2016.
- [18] F. D. Munoz and J.-P. Watson, "A scalable solution framework for stochastic transmission and generation planning problems," *Computational Management Science*, vol. 12, pp. 491–518, October 2015.

- [19] J. Zou, S. Ahmed, and X. A. Sun, "Nested Decomposition of Multistage Stochastic Integer Programs with Binary State Variables," 2016, working Paper.
- [20] M. V. F. Pereira and L. M. V. G. Pinto, "Multi-stage stochastic optimization applied to energy planning," *Mathematical Programming*, vol. 52, pp. 359–375, May 1991.
- [21] P. Ahlhaus and P. Stursberg, "Transmission Capacity Expansion: An Improved Transport Model," in *2013 4th IEEE/PES Innovative Smart Grid Technologies Europe (ISGT EUROPE)*. Lyngby, Denmark: Institute of Electrical and Electronics Engineers, 6–9 October 2013.
- [22] S. Succar and R. H. Williams, "Compressed Air Energy Storage Theory, Resources, And Applications For Wind Power," Princeton Environmental Institute, Tech. Rep., April 2008.
- [23] F. Graves, T. Jenkin, and D. Murphy, "Opportunities for Electricity Storage in Deregulating Markets," *The Electricity Journal*, vol. 12, pp. 46–56, October 1999.
- [24] R. Sioshansi, P. Denholm, T. Jenkin, and J. Weiss, "Estimating the Value of Electricity Storage in PJM: Arbitrage and Some Welfare Effects," *Energy Economics*, vol. 31, pp. 269–277, March 2009.
- [25] X. Xi and R. Sioshansi, "A Dynamic Programming Model of Energy Storage and Transformer Deployments to Relieve Distribution Constraints," *Computational Management Science*, vol. 13, pp. 119–146, January 2016.
- [26] R. T. Rockafellar and R. J.-B. Wets, "Scenario and policy aggregation in optimization under uncertainty," *Mathematics of Operations Research*, vol. 16, pp. 119–147, November 1991.
- [27] D. Gade, G. Hackebeil, S. M. Ryan, J.-P. Watson, R. J.-B. Wets, and D. L. Woodruff, "Obtaining lower bounds from the progressive hedging algorithm for stochastic mixed-integer programs," *Mathematical Programming*, vol. 157, pp. 47–67, May 2016.
- [28] Y. Liu, "Electricity Capacity Investments and Cost Recovery with Renewables," Ph.D. dissertation, The Ohio State University, Columbus, Ohio, USA, August 2016.
- [29] *Annual Energy Outlook 2014*, DOE/EIA-0383 (2014) ed., U.S. Energy Information Administration, April 2014.
- [30] T. Mai, D. Sandor, R. Wisner, and T. R. Schneider, "Renewable Electricity Futures Study: Executive Summary," National Renewable Energy Laboratory, Golden, Colorado, Tech. Rep. NREL/TP-6A20-52409-ES, 2012.
- [31] A. Lopez, B. Roberts, D. Heimiller, N. Blair, and G. Porro, "U.S. Renewable Energy Technical Potentials: A GIS-Based Analysis," National Renewable Energy Laboratory, Golden, Colorado, Tech. Rep. NREL/TP-6A20-51946, July 2012.
- [32] Y. Liu, M. C. Roberts, and R. Sioshansi, "A Vector Autoregression Weather Model for Electricity Supply and Demand Modeling," 2017, working paper.
- [33] M. Muratori, M. C. Roberts, R. Sioshansi, V. Marano, and G. Rizzoni, "A highly resolved modeling technique to simulate residential power demand," *Applied Energy*, vol. 107, pp. 465–473, July 2013.
- [34] A. Pielow, R. Sioshansi, and M. C. Roberts, "Modeling Short-run Electricity Demand with Long-term Growth Rates and Consumer Price Elasticity in Commercial and Industrial Sectors," *Energy*, vol. 46, pp. 533–540, October 2012.
- [35] J.-P. Watson and D. L. Woodruff, "Progressive hedging innovations for a class of stochastic mixed-integer resource allocation problems," *Computational Management Science*, vol. 8, pp. 355–370, November 2011.



Ramteen Sioshansi (M'11–SM'12) holds the B.A. degree in economics and applied mathematics and the M.S. and Ph.D. degrees in industrial engineering and operations research from the University of California, Berkeley, and an M.Sc. in econometrics and mathematical economics from The London School of Economics and Political Science.

He is an associate professor in the Department of Integrated Systems Engineering at The Ohio State University, Columbus, OH. His research focuses on renewable and sustainable energy system analysis and the design of restructured competitive electricity markets.



Antonio J. Conejo (F'04) received the M.S. degree from the Massachusetts Institute of Technology, Cambridge, MA, in 1987, and the Ph.D. degree from the Royal Institute of Technology, Stockholm, Sweden, in 1990.

He is currently a full professor in the Department of Integrated Systems Engineering and the Department of Electrical and Computer Engineering, The Ohio State University, Columbus, OH. His research interests include control, operations, planning, economics and regulation of electric energy systems, as well as statistics and optimization theory and its applications.



Yixian Liu holds the B.E. degree in logistics engineering from Tianjin University and the M.S. and Ph.D. degrees in industrial and systems engineering from The Ohio State University.

Her Ph.D. work focuses on weather forecasting, electricity capacity investment, and energy-policy analysis.